

General Procedure for the Reaction of α -Thiocarbanions with Iron Pentacarbonyl. To the sulfide (4.0 mmol) in anhydrous THF (30 mL) at -78°C was added, drop-by-drop, 1 equiv of RLi or LDA. After the solution was stirred for 1 h (solution became yellow), iron pentacarbonyl (4.0 mmol) was added and the reaction mixture was stirred for 2 h either at -78°C or while being warmed up to room temperature (see Table I). Then the electrophile (4.0 mmol in the case of RLi; 8.0 mmol for LDA) was added, and stirring was continued overnight. The reaction mixture was then concentrated by flash evaporation, and the resulting crude products were separated by first filtering through a short column of silica gel (CH_2Cl_2 -ethyl acetate) and then by silica gel thin-layer chromatography (hexane-ethyl acetate).

Products. 7, R = R' = Ph: IR $\nu(\text{CO})$ 1685 cm^{-1} ; $^1\text{H NMR}$ (CDCl_3) δ 2.18 (s, 3 H, CH_3), 4.97 (s, 1 H, CH), 7.40 (s (br), 10 H, Ph); MS m/e 242 $[\text{M}]^+$, 199 $[\text{M} - \text{COCH}_3]^+$; mp $64-65^\circ\text{C}$ (lit.¹³ mp $64-66^\circ\text{C}$). Anal. Calcd for $\text{C}_{16}\text{H}_{14}\text{OS}$: C, 74.36; H, 5.83; S, 13.20. Found: C, 74.18; H, 5.85; S, 12.81.

7, R = $p\text{-CH}_3\text{C}_6\text{H}_4$, R' = Ph: IR $\nu(\text{CO})$ 1690 cm^{-1} ; $^1\text{H NMR}$ (CDCl_3) δ 2.11, 2.25 (s each, 6 H, two methyl groups), 4.91 (s, 1 H, CH), 6.97 (d, 2 H, $J = 8$ Hz, protons on carbon ortho to sulfur bearing carbon), 7.22 (d, 2 H, $J = 8$ Hz, protons on carbon meta to sulfur bearing carbon), 7.27 (s, 5 H, Ph); MS m/e 256 $[\text{M}]^+$,

213 $[\text{M} - \text{COCH}_3]^+$; mp $71-73^\circ\text{C}$. Anal. Calcd for $\text{C}_{16}\text{H}_{16}\text{OS}$: C, 74.96; H, 6.29; S, 12.51. Found: C, 74.60; H, 6.57; S, 12.93.

7, R = $p\text{-CH}_3\text{OC}_6\text{H}_4$, R' = Ph: IR $\nu(\text{CO})$ 1685 cm^{-1} ; $^1\text{H NMR}$ (CDCl_3) δ 2.16 (s, 3 H, CH_3), 3.72 (s, 3 H, OCH_3), 4.87 (s, 1 H, CH), 6.70-7.40 (m, 9 H, aromatic protons); MS m/e 270 $[\text{M}]^+$, 239 $[\text{M} - \text{OCH}_3]^+$, 227 $[\text{M} - \text{COCH}_3]^+$. Anal. Calcd for $\text{C}_{16}\text{H}_{16}\text{O}_2\text{S}$: C, 70.63; H, 5.92; S, 11.77. Found: C, 70.81; H, 6.11; S, 11.43.

Products 8-10 were identified by comparison of spectral data with those described in the literature and, in some cases, by comparison with authentic materials.

Acknowledgment. We are grateful to the Natural Sciences and Engineering Research Council for support of this research.

Registry No. 7 (R = R' = Ph), 10371-49-0; 7 (R = $p\text{-CH}_3\text{C}_6\text{H}_4$, R' = Ph), 81602-64-4; 7 (R = Ph, R' = C_6H_5), 77119-58-5; 7 (R = $p\text{-CH}_3\text{OC}_6\text{H}_4$, R' = Ph), 81602-65-5; 8 (R = R' = Ph), 53104-99-7; 8 (R = $p\text{-CH}_3\text{C}_6\text{H}_4$, R' = Ph), 76160-89-9; 8 (R = $p\text{-CH}_3\text{OC}_6\text{H}_4$, R' = Ph), 81602-66-6; 9 (R' = Ph), 588-59-0; 10 (R = Ph, R'' = CH_3), 934-87-2; 10 (R = R'' = Ph), 884-09-3; 10 (R = Ph, R'' = $\text{CH}(\text{CH}_3)_2$), 58443-71-3; 10 (R = Ph, R'' = $\text{CH}_2\text{CH}=\text{CH}$), 25542-72-7; 10 (R = Ph, R'' = $\text{C}_6\text{H}_5\text{O}$), 17357-38-9; 10 (R = $p\text{-CH}_3\text{OC}_6\text{H}_4$, R'' = Ph), 24197-73-7; $\text{Fe}(\text{CO})_5$, 13463-40-6; PhSCH_2Ph , 831-91-4; $p\text{-CH}_3\text{C}_6\text{H}_4\text{SCH}_2\text{Ph}$, 5023-60-9; $\text{PhSCH}_2\text{CH}=\text{CH}_2$, 5296-64-0; $p\text{-CH}_3\text{OC}_6\text{H}_4\text{SCH}_2\text{Ph}$, 26905-24-8.

(13) Newman, H.; Angier, R. B. *Tetrahedron* 1970, 26, 825.

Aspects of the Chemistry of Substituted Ruthenium Clusters Involving Bis(diphenylphosphino)- or Bis(diphenylarsino)methane as Bridging Ligands. Reactivity toward Hydrogen and Potential Applications in Catalysis. Crystal and Molecular Structure of $(\mu\text{-H})_2\text{Ru}_3(\text{CO})_6(\mu\text{-P}(\text{C}_6\text{H}_5)\text{CH}_2\text{P}(\text{C}_6\text{H}_5)_2)_2$ and $(\mu\text{-H})_2\text{Ru}_3(\text{CO})_6(\mu\text{-As}(\text{C}_6\text{H}_5)\text{CH}_2\text{As}(\text{C}_6\text{H}_5)_2)_2$

Guy Lavigne, Noël Lukan, and Jean-Jacques Bonnet*

Laboratoire de Chimie de Coordination du CNRS Associé à l'Université Paul Sabatier, 31400 Toulouse, France

Received February 25, 1982

Reaction of $\text{Ru}_3(\text{CO})_8(\text{dppm})_2$ (**1a**) (dppm = bis(diphenylphosphino)methane) with molecular hydrogen at 85°C gives the trinuclear dihydrido cluster complex $(\mu\text{-H})_2\text{Ru}_3(\text{CO})_6(\mu\text{-P}(\text{C}_6\text{H}_5)\text{CH}_2\text{P}(\text{C}_6\text{H}_5)_2)_2$ (**3a**) in high yield and purity. Under the same experimental conditions, $\text{Ru}_3(\text{CO})_8(\text{dpam})_2$ (**1b**) (dpam = bis(diphenylarsino)methane) provides the intermediate monohydrido species $(\mu\text{-H})\text{Ru}_3(\text{CO})_7(\mu\text{-As}(\text{C}_6\text{H}_5)\text{CH}_2\text{As}(\text{C}_6\text{H}_5)_2)(\text{dpam})$ (**2b**) which further reacts with H_2 at 120°C , yielding the dihydrido cluster complex $(\mu\text{-H})_2\text{Ru}_3(\text{CO})_6(\mu\text{-As}(\text{C}_6\text{H}_5)\text{CH}_2\text{As}(\text{C}_6\text{H}_5)_2)_2$ (**3b**). The crystal and molecular structures of **3a** and **3b** are reported. Crystal data for **3a**: monoclinic, space group C_2/c ; $a = 14.510$ (2) Å, $b = 16.533$ (1) Å, $c = 18.198$ (2) Å, $\beta = 90.80$ (1) $^\circ$; current $R = 0.026$, $R_w = 0.028$ from 5151 reflections with $F_o > 3\sigma(F_o)$. Crystal data for **3b**: monoclinic, space group $P2_1/c$; $a = 14.726$ (5) Å, $b = 16.931$ (7) Å, $c = 18.097$ (4) Å, $\beta = 92.40$ (2) $^\circ$; current $R = 0.041$, $R_w = 0.039$ from 3565 reflections. Both structures consist of a triangular array of Ru atoms (isosceles in **3a**) involving two equatorial CO ligands per metal atom; both cluster faces are capped in a similar way by identical ligand units $\mu\text{-X}(\text{C}_6\text{H}_5)\text{CH}_2\text{X}(\text{C}_6\text{H}_5)_2$ ($\text{X} = \text{P}$ or As). In a typical ligand unit, the first P (or As) atom bridges a metal-metal edge, while the second one is coordinated to the third metal atom. The two hydrido ligands are found to bridge inequivalent metal-metal bonds. This feature is confirmed by $^1\text{H NMR}$ data, including variable-temperature experiments. Acidification of the reported complexes gives new cationic trihydrido cluster complexes which are characterized by $^1\text{H NMR}$. Catalytic tests show that complex **3a** catalyzes the hydrogenation of cyclohexane to cyclohexanol (86% conversion after 18 h, using a 1/1000 catalyst/substrate ratio; $t = 90^\circ\text{C}$; $P(\text{H}_2) = 100$ bar).

Introduction

Earlier work in this laboratory has led to the isolation of the new cluster complexes $\text{Ru}_3(\text{CO})_8\text{L}_2$ (**1**) stabilized by bridging bis(diphenylphosphino)methane¹ or bis(di-

phenylarsino)methane ligands (**1a**, L = dppm, **1b**, L = dpam). In attempts to determine whether or not such species could be efficient catalyst precursors, we were prompted to investigate the nature of the complexes which could be generated under the conditions of a typical hydrogenation reaction. We were led to these studies through previous reports²⁻¹¹ dealing with some versatile effects of

(1) Lavigne, G.; Bonnet, J.-J. *Inorg. Chem.* 1981, 20, 2713.

phosphine addition in catalytic systems involving cluster participation.

Our previous observations¹ revealed that the complex $\text{Ru}_3(\text{CO})_8(\text{dppm})_2$ (**1a**) experiences a facile thermal transformation via a stepwise oxidative cleavage of a coordinated dppm ligand, yielding $\text{Ru}_3(\text{CO})_7(\mu_3\text{-P}(\text{C}_6\text{H}_5)(\mu\text{-CHP}(\text{C}_6\text{H}_5)_2)(\text{dppm}))$ as a final product.¹² In contrast, **1a** and **1b** were found to react with molecular oxygen without oxidative cleavage of the bridging ligand, affording the trinuclear oxo derivative $\text{Ru}_3(\mu_3\text{-O})(\text{CO})_6(\text{L})_2$.¹³ Following these observations as well as previous ones,¹⁴ the oxidative cleavage of phosphine or arsine ligands could be expected to occur finally in absence of an energetically more favorable reaction.

When attempting the reaction of **1** with molecular hydrogen, we had in mind a closely related experiment¹⁵ concerning $\text{Ru}_3(\text{CO})_{12}$ and $\text{Os}_3(\text{CO})_{12}$, which provided $\text{H}_4\text{Ru}_4(\text{CO})_{12}$ and $\text{H}_2\text{Os}_3(\text{CO})_{10}$, respectively. We first hoped that an imposed retention of the trinuclear ruthenium frame by edge-bridging ligands could favor the formation of substituted analogues of the very attractive species $\text{H}_2\text{Os}_3(\text{CO})_{10}$ which is still unknown in the chemistry of ruthenium.¹⁶ However, different results have been obtained, since an oxidative cleavage of phosphine or arsine ligands has proved to be concomitant with the addition of hydrogen, leading to new hydrido cluster complexes which were characterized by spectroscopic and crystallographic techniques. Preliminary catalytic runs show that these complexes have moderate efficiency in a catalytic hydrogenation reaction.

Experimental Section

Synthetic Work. The compounds reported in this study do not exhibit particular sensitivity to air at room temperature. However, as a matter of routine in this laboratory, the reactions were performed under an atmosphere of prepurified nitrogen using Schlenk tubes and vacuum lines. Organic solvents were degassed prior to use. $\text{Ru}_3(\text{CO})_{12}$ ¹⁷ and $\text{Ru}_3(\text{CO})_8(\text{dppm})_2$ (**1a**)¹ were prepared by published procedures. $\text{Ru}_3(\text{CO})_8(\text{dpam})_2$ (**1b**) can be obtained through the same experimental conditions as those stated for the phosphorus derivative.¹ Complexes **1a** and **1b** were purified on a silica gel column (benzene as eluent) and recrystallized from an acetone/ethanol medium. Molecular hydrogen was allowed to bubble into xylene solutions of these complexes at atmospheric pressure and variable temperatures.

Spectroscopic Data. IR Spectra. Solution spectra in the

$\nu(\text{CO})$ region were recorded on a Perkin-Elmer 225 spectrophotometer.

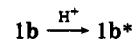
NMR Spectra. ¹H NMR spectra were recorded on a Bruker WH90 Fourier transform spectrometer. Since no ³¹P-spin decoupler was available on this apparatus, the molecular structure of the complexes was elucidated from arsine derivatives. Chemical shifts, δ , given in this paper are relative to internal Me_4Si reference. All ¹H NMR spectra were recorded at 90 MHz, using CD_2Cl_2 as solvent. The variable-temperature experiment was carried out in deuterated toluene. Complete NMR data are displayed in Table XI.

Preparation of $(\mu\text{-H})_2\text{Ru}_3(\text{CO})_6(\mu\text{-P}(\text{C}_6\text{H}_5)\text{CH}_2\text{P}(\text{C}_6\text{H}_5)_2)_2$ (3a**).** In a typical experiment, 350 mg of $\text{Ru}_3(\text{CO})_8(\text{dppm})_2 \cdot 2(\text{CH}_3)_2\text{CO}$ (**1a**) as crystals was dissolved in 30 mL of xylene. A continuous hydrogen stream was allowed to bubble into this solution. The temperature was raised to 80–85 °C for 90 min: the initial red solution turned gold yellow. The solution was cooled and concentrated under vacuum. Elution with dichloromethane/hexane mixtures afforded a yellow band as the only detectable product. Recrystallization from a 1/1 dichloromethane/hexane solution gave 210 mg of crystals (77 % yield) which were directly suitable for X-ray analysis: IR ($\nu(\text{CO})$, CH_2Cl_2 solution) 2032 (m), 2000 (s), 1975 (s), 1940 (m), 1915 (m) cm^{-1} ; ¹H NMR (CD_2Cl_2 solution) δ 4.78 (broad methylene resonance), 3.47 (broad methylene resonance), -15.87 (hydride signal), -19.35 (hydride signal). Anal. Calcd for $(\mu\text{-H})_2\text{Ru}_3(\text{CO})_6(\mu\text{-P}(\text{C}_6\text{H}_5)\text{CH}_2\text{P}(\text{C}_6\text{H}_5)_2)_2$ ($\text{C}_{44}\text{H}_{36}\text{O}_6\text{P}_2\text{Ru}_3$): C, 48.58; H, 3.33. Found: C, 48.20; H, 3.30. Evidence for benzene evolution in this reaction was obtained through the synthesis of **3a** by using 2-ethoxyethanol as a benzene-free solvent: gas chromatography of the reaction mixture was performed on an Intersmat IGC 121 DFL apparatus equipped with a flame ionization detector, using a 3.0 m \times 0.33 cm column packed with 10% SE 30 on Chromosorb PAW 80/100. In a typical experiment, 1.3 mol of C_6H_6 per mole of starting material (**1a**) could be detected. (Note that the high insolubility of **3a** in 2-ethoxyethanol at room temperature allows direct crystallization of this complex upon cooling, providing a clean recovery. This solvent can be favorably used in all the syntheses reported here).

Preparation of $(\mu\text{-H})\text{Ru}_3(\text{CO})_7(\mu\text{-As}(\text{C}_6\text{H}_5)\text{CH}_2\text{As}(\text{C}_6\text{H}_5)_2)(\text{dpam})\text{-CH}_2\text{Cl}_2$ (2b**).** The reaction of **1b** with molecular hydrogen was carried out under the same above conditions (xylene solution, 90 min, 80–85 °C, continuous hydrogen stream). Although no change in the initial red color was observed, the IR spectrum gave evidence for the formation of a new species. Chromatographic workup on silica gel (benzene as eluent) gave a red compound. Recrystallization from dichloromethane/petroleum ether afforded red crystals which were subsequently formulated as $(\mu\text{-H})\text{Ru}_3(\text{CO})_7(\mu\text{-As}(\text{C}_6\text{H}_5)\text{CH}_2\text{As}(\text{C}_6\text{H}_5)_2)(\text{dpam})\text{-CH}_2\text{Cl}_2$ (**2b**) (yield ~50%): IR ($\nu(\text{CO})$, CH_2Cl_2 solution) 2030 (s), 1975 (br), 1920 (m) cm^{-1} ; ¹H NMR (CD_2Cl_2 solution) δ 4.64 (s, CH_2), 2.24 (q, CH_2), -14.56 (s, hydride signal). The intermediate nature of this species was established by the following experiment.

Preparation of $(\mu\text{-H})_2\text{Ru}_3(\text{CO})_6(\mu\text{-As}(\text{C}_6\text{H}_5)\text{CH}_2(\text{C}_6\text{H}_5)_2)_2$ (3b**).** Crystals of **2b** were dissolved in xylene and molecular hydrogen was allowed to bubble into the solution for 3 h at 120 °C: the initial red colour turned yellow. The solution was concentrated and chromatographed; elution with benzene gave no traces of **2b**; further elution with dichloromethane/hexane afforded a new compound, **3b**, which was recrystallized from 1/1 dichloromethane/hexane as yellow crystals which can be formulated as $(\mu\text{-H})_2\text{Ru}_3(\text{CO})_6(\mu\text{-As}(\text{C}_6\text{H}_5)\text{CH}_2\text{As}(\text{C}_6\text{H}_5)_2)_2$ (**3b**) (yield ~60%): IR ($\nu(\text{CO})$, CH_2Cl_2 solution) 2037 (m), 2005 (s), 1980 (s), 1940 (m), 1920 (m) cm^{-1} ; ¹H NMR (CD_2Cl_2 solution) δ 4.74 (q, CH_2), 3.13 (quartet with superimposing hydride coupling, CH_2), -16.08 (doublet of doublets, hydride signal), -20.11 (d, hydride signal).

Preparation of Cationic Hydrido Cluster Complexes. Acidification of various complexes reported here led to the formation of new cationic cluster complexes which were fully characterized from their ¹H NMR spectra. These experiments were realized by adding an excess of trifluoroacetic acid to dichloromethane solutions of the complexes at room temperature.



(2) Chini, P.; Martinengo, S.; Garlaschelli, G. *J. Chem. Soc., Chem. Commun.* 1972, 709.

(3) Ryan, R. C.; Pittman, C. U., Jr.; O'Connor, J. P. *J. Am. Chem. Soc.* 1977, 99, 1986.

(4) Sanchez-Delgado, R. A.; Bradley, J. S.; Wilkinson, G. *J. Chem. Soc. Dalton Trans.* 1976, 1399.

(5) Labroue, D.; Poilblanc, R. *J. Mol. Catal.* 1977, 2, 329.

(6) Vaglio, G. A.; Valle, M. *Inorg. Chim. Acta* 1978, 30, 161.

(7) Frediani, P.; Matteoli, U.; Bianchi, M.; Piacenti, F.; Menchi, G. *J. Organomet. Chem.* 1978, 150, 273.

(8) Pittman, C. U., Jr.; Wilemont, G. M.; Wilson, W. D.; Ryan, R. C. *Angew. Chem., Int. Ed. Engl.* 1980, 19, 478.

(9) Brown, S. C.; Evans, J. *J. Organomet. Chem.* 1980, 194.

(10) Reimann, W.; Abboud, W.; Basset, J. M.; Mutin, R.; Rempel, G. L.; Smith, A. K. *J. Mol. Catal.* 1980, 9, 349 and references therein.

(11) Bianchi, M.; Matteoli, U.; Menchi, G.; Frediani, P.; Botteghi, C. *J. Organomet. Chem.* 1980, 195, 337.

(12) New intermediate species have now been isolated in this reaction (Lavigne G.; Bonnet, J.-J., in preparation).

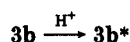
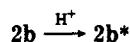
(13) Lavigne G.; Lugan, N.; Bonnet, J.-J. *Nouv. J. Chim.* 1981, 5, 423.

(14) Fahey, D. R.; Mahan, J. E. *J. Am. Chem. Soc.* 1976, 98, 4499.

(15) Knox, S. A. R.; Koepke, J. W.; Andrews, M. A.; Kaesz, H. D. *J. Am. Chem. Soc.* 1975, 97, 709.

(16) A small number of polynuclear metal carbonyl derivatives are known which are formally unsaturated in that multiple metal-metal bonds are present. For example, see: Mays, M. J.; Prest, D. W.; Raithby, P. R. *J. Chem. Soc.* 1980, 171 and references therein. See also: Ciani, G.; D'Alfonso, G.; Freni, M.; Romiti, P.; Sironi, A.; Albinati, A. *J. Organomet. Chem.* 1977, 136, C49.

(17) Mantovani, A.; Cenini, S. *Inorg. Synth.* 1900, 16, 47.



$[(\mu-H)Ru_3(CO)_8(dpam)_2]^+$ (**1b***): 1H NMR (CD_2Cl_2 solution): δ 4.57 (s, CH_2), -19.45 (s, hydride signal). $[(\mu-H)_2Ru_3(CO)_7(\mu-As(C_6H_5)CH_2As(C_6H_5)_2)(dpam)]^+$ (**2b***): 1H NMR (CD_2Cl_2 solution) δ 4.06 (quartet with superimposed hydride coupling, CH_2), 2.93 (q, CH_2), -14.05 (d, hydride signal), -18.49 (doublet of doublets, hydride signal). $[(\mu-H)_3Ru_3(CO)_6(\mu-As(C_6H_5)CH_2As(C_6H_5)_2)_2]^+$ (**3b***): 1H NMR (CD_2Cl_2 solution) δ 3.75 (quartet with superimposed hydride coupling, CH_2), -16.18 (d, hydride signal $\times 2$), -19.43 (s, hydride signal).

Catalytic Tests. Preliminary catalytic runs were performed by using a Sotalem 150b rocking autoclave. Tetrahydrofuran was freshly distilled on Na/benzophenone prior to use. In a typical experiment, 35 mL of THF, 50 mg of **3a** (0.046 mmol), and 5 mL of cyclohexanone (48.2 mmol) (molar ratio, catalyst/cyclohexanone ca. 1/1000) were introduced into the autoclave under argon. The temperature was raised to $90 \pm 1^\circ C$ (stabilization required 15 min). A pressure of 100 bars of hydrogen was then supplied. Reactions were quenched at desired times by rapid cooling and the products immediately analyzed by GC (Intersmat IGC 121 DFL equipped with a 1.5-m column containing Carbowax 20M on Chromosorb PAW 60/80).

Collection and Reduction of X-ray Data. **A.** Compound **3a**. Preliminary Laue and precession photographs showed **3a** to crystallize in a monoclinic cell. Systematic extinctions (hkl , $h + k = 2n + 1$; $h0l$, $l = 2n + 1$) were consistent with space groups C_{2h}^2-C2/c and C_s^4-Cc . The structure was successfully solved in the centric space group $C2/c$. The crystal selected for data collection was a truncated parallelepiped with boundary planes of the forms $\{211\}$, $\{1\bar{1}1\}$, $\{001\}$, and $\{111\}$; the distances from these faces to an arbitrary origin in the crystal were respectively 0.069, 0.194, 0.126, and 0.216 mm, the crystal volume being equal to 0.016 mm^3 . The setting angles of 25 reflections with $24^\circ < 2\theta(Mo K\alpha) < 26^\circ$ were refined by least-squares procedures which led to the cell constants. These constants and other pertinent data are listed in Table I. Intensity data were collected by using an Enraf Nonius CAD4 diffractometer. A total of 7376 intensities were recorded out to $2\theta(Mo) < 56^\circ$. These intensities were corrected for Lorentz, polarization, and absorption effects¹⁸ and reduced to observed structure factor amplitudes by using a p value of 0.03.¹⁹ Only 5151 unique reflections having $F_o^2 > 3\sigma(F_o^2)$ were used in subsequent calculations after processing.

B. Compound 3b. Preliminary film data revealed that crystals of **3b** belong to the monoclinic system and show systematic extinctions ($0k0$, $k = 2n + 1$; $h0l$, $l = 2n + 1$) consistent with space group $C_{2h}^5-P2_1/c$. Cell constants were obtained as described above. Crystal data are presented in Table IB. A total of 6514 reflections were recorded up to $2\theta(Mo) = 40^\circ$. Intensity data were processed under routine conditions (vide supra) (Note that absorption corrections could not be computed in this case, owing to the poor shape of the crystal.) Finally, 3565 reflections with $F_o^2 > 3\sigma(F_o^2)$ were used in subsequent calculations.

Solution and Refinement of the Structures

A. Compound 3a. The structure was solved by the heavy-atom technique.¹⁸ The positions of Ru atoms were obtained from a conventional Patterson synthesis. Subsequent refinements and difference Fourier calculations led to the location of all other non-hydrogen atoms. Let us mention a feature concerning the location of the two CO ligands coordinated to Ru(1): these ligands should be related through the twofold axis symmetry, since Ru(1) is located on the C_2 axis. However, a difference Fourier synthesis showed a splitting of the peaks associated with the electron density

of the corresponding carbon and oxygen atoms; the magnitude of these peaks was equal to half of the expected electron density. These features were consistent with a statistical distribution of the two CO ligands between four sites labelled as C(1)O(1), C(1b)O(1b), C(1)*O(1)*, and C(1b)*O(1b)* (starred atoms are in equivalent position $1 - x, y, 1/2 - z$). The separation of these sites (C(1)---C(1b) = 0.8 ; O(1)---O(1b) = 1.2 ) allowed a satisfactory refinement of the corresponding atomic coordinates, by using fixed occupancy factors of 0.5.

To ascertain our choice of the centric space group $C2/c$, we tried to refine the structure in the alternative acentric space group Cc . Removal of the C_2 rotation axis, when going from $C2/c$ to Cc , might avoid the disorder problem or, at least, might lead to different occupancy factors for the disordered carbonyl groups. However, a difference Fourier map calculated after one cycle of refinement in the Cc group of a model including the whole molecule but the disordered atoms showed again a splitting of carbon and oxygen atoms coordinated to Ru(1), clearly indicating that the observed disorder was not induced by the C_2 axis. The corresponding peaks were found to have the same position and intensity as in the centric space group $C2/c$. Consequently, no further attempts to refine the structure in space group Cc were made.

Atomic scattering factors were taken from Cromer and Waber's tabulation²⁰ for all atoms but hydrogen, for which the values of Stewart et al. were used.²¹ Anomalous dispersion terms for Ru and P atoms were included in F_c .²² Full-matrix least-squares refinement of a model including all non-hydrogen atoms with anisotropic thermal parameters yielded values for R and R_w on F of 0.034 and 0.046, respectively. A subsequent Fourier difference map allowed the location of all hydrogen atoms: two of the three highest peaks in this map could be assigned to the hydrogen atoms of the methylene group; the third one, of equal intensity, was located on the C_2 axis, giving a reasonable position for a μ -hydride ligand bridging the metal-metal vector Ru(2)-Ru(2)* (Ru(2)-H(1) = Ru(2)*-H(1) = 1.81 ). Let us note that a residual peak of magnitude equal to half the preceding one was found close to the idealized position expected for the second μ -hydride ligand H(2) bridging the metal-metal vector Ru(1)-Ru(2) (further discussion concerning this hydride ligand is given later in this paper). All hydrogen atoms were introduced in fixed position; no attempts to refine the hydride positions was made.²³ A B value of 4 ² was assigned to hydride ligands. The hydrogen atoms of phenyl rings were introduced in idealized position (C-H = 0.95 ); the isotropic thermal parameters of these atoms were taken as 1 ² greater than those of their neighbor carbon atoms. The final cycle of refinement, including an isotropic secondary extinction correction,²⁴ led to $R(F) = 0.026$ and $R_w(F) = 0.029$.

In regard to the alternative possibility of space group Cc discussed above, additional features give now evidence that the correct space group has been used: (i) the low values of R and R_w are satisfactory; (ii) all vibrational ellipsoids are quite normal; (iii) the fact that all hydrogen atoms could be located in difference Fourier maps clearly indicates that the crystallographic C_2 symmetry even extends to the light atoms.

Final positional and thermal parameters of all atoms are listed in Table II. Table III contains the root-mean-square amplitudes of vibration.²⁵ A complete listing of observed and calculated structure factor amplitudes is available.²⁵

B. Compound 3b. A conventional Patterson synthesis proved to be closely similar to that observed for **3a**. Accordingly, ap-

(20) Cromer, D. T.; Waber, J. T. "International Tables for X-ray Crystallography"; Kynoch Press: Birmingham, England, 1974; Vol. IV, Table 2.2A.

(21) Stewart, R. F.; Davidson, E. R.; Simpson, W. T. *J. Chem. Phys.* 1965, 42, 3175.

(22) Cromer, D. T.; Waber, J. T. "International Tables for X-ray Crystallography"; Kynoch Press: Birmingham, England, 1974; Vol. IV, Table 2.3.1.

(23) The observed residual peaks in this structure allowed an approximate location of hydride ligands. Nevertheless, it was not found reasonable to refine these positions since metal-hydrogen bonding distances may be underestimated in X-ray structure determinations.

(24) (a) Zachariasen, W. H. *Phys. Rev. Lett.* 1967, 18, 195. (b) *Acta Crystallogr.* 1967, 23, 558.

(25) See paragraph at the end of the paper regarding supplementary material.

(18) The main programs used were the following: The Northwestern absorption program, AGNOST, which includes the Coppens-Leiserowitz-Rabinovich logic for Gaussian integration and the Tompa De Meulenaer analytical method; Zalkin's FORDP Fourier summation program; Johnson's ORTEP; Busing's and Levy's ORFFE error function program; Ibers' NUCLS full-matrix least-squares program, which in its nongroup form closely resembles the Busing-Levy ORFLS program.

(19) Moeset, A.; Bonnet, J.-J.; Galy, J. *Acta Crystallogr., Sect. B* 1977, B33, 2639.

Table I. Experimental Data for X-ray Diffraction Studies

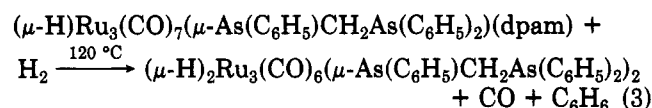
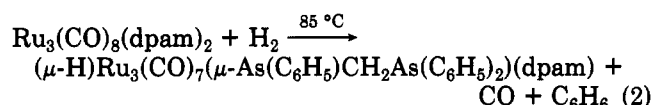
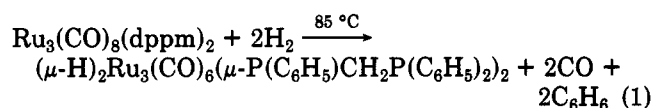
	A	B
Crystal Data		
compd	3a	3b
formula	C ₄₄ H ₃₆ O ₆ P ₄ Ru ₃	C ₄₄ H ₃₆ O ₆ As ₄ Ru ₃
fw, amu	1087.87	1263.66
cryst system	monoclinic	monoclinic
space group	C2/c	P2 ₁ /c
a, Å	14.510 (2)	14.726 (5)
b, Å	16.553 (1)	16.931 (7)
c, Å	18.198 (2)	18.097 (4)
β, deg.	90.80 (1)	92.40 (2)
V, Å ³	4370	4508
D, g·cm ⁻³	1.652	1.862
μ, cm ⁻¹	11.9	40.9
Intensity Data		
radiation	Mo Kα (λ = 0.709 30 Å) from monochromator	Mo Kα from monochromator
takeoff angle, deg	3.5	3.2
2θ limits, deg	3-56	3-40
scan mode	ω/0.67θ	ω/2θ
scan range	0.9° below Kα ₁ to 0.9° above Kα ₂	0.9° below Kα ₁ to 0.9° above Kα ₂
ω scan speed, deg/min	1.5	2
reflectns collected	7376	6514
unique data used	5151 F _o ² > 3σ(F _o) ²	3565 F _o ² > 3σ(F _o) ²
final no. of variables	277	262
R = Σ F _o - F _c /Σ F _o	0.026	0.041
R _w = [Σw(F _o - F _c) ² /ΣwF _o ²] ^{1/2}	0.028	0.039
std error in an observn of unit weight	1.55 e	1.72 e

proximate atomic coordinates of all atoms were obtained from the previous model through the following translation: Δx ≈ 0.25; Δy ≈ 0.25; Δz ≈ 0, leading to a structure with all atoms in general positions. The main difference with the previous model 3a was the absence of any disorder of carbonyl ligands in this case. Owing to the large number of atoms in this structure, phenyl rings were refined as rigid groups (imposed D_{6h} symmetry; C-C = 1.395 Å; C-H = 0.95 Å). Although a final Fourier difference map allowed an approximate location of hydride ligands, these atoms were not included in the model.

The final cycle of refinement led to convergence factors R = 0.041 and R_w = 0.039. Final values of positional and thermal parameters of all independent atoms are listed in Table IV; those of rigid groups are in Table V.²⁵ The root mean squares amplitudes of vibration are presented in Table VI.²⁵ A listing of observed and calculated structure factor amplitudes is available.²⁵

Results and Discussion

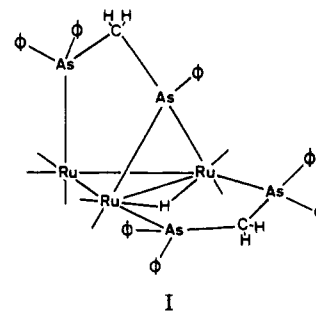
Syntheses of 3a, 2b, and 3b. Owing to the absence of any detectable side product, the reaction of 1a and 1b with molecular hydrogen is a very clean one. It can be schematized as shown in eq 1-3.



This reaction scheme reveals three salient features: (i) the triangular framework of ruthenium atoms is retained throughout the reaction with hydrogen, whereas an increased nuclearity was previously observed¹⁵ for Ru₃(CO)₁₂, providing H₄Ru₄(CO)₁₂; (ii) both clusters 1a and 1b exhibit an increased affinity for molecular hydrogen in comparison with Ru₃(CO)₁₂ since the reactions work under milder

conditions: (iii) the hydrogen uptake is concomitant with an oxidative addition of coordinated dppm or dpam ligands to the clusters and proceeds in two steps; it provides a satisfactory control of the oxidative addition of these ligands, since no further cleavage is observed in refluxing xylene.

The intermediate monohydride species 2b has been isolated from the arsine derivative. An accurate structural study of this complex (both X-ray and neutron diffraction experiments) will be published elsewhere.²⁶ A scheme of this structure is given I.



A dpam ligand is still bridging two ruthenium atoms, as referred to the parent complex 1b, while the activation of the second ligand led to the formation of the μ-As-(C₆H₅)CH₂As(C₆H₅)₂ fragment in a face capped position. The final step of the reactions with molecular hydrogen is illustrated by structures 3a and 3b which are described (vide infra).

Description of the Structures of 3a and 3b. A. Structure of 3a. The crystal structure of 3a consists of the packing of four trinuclear molecules per unit cell separated by normal van der Waals distances. Figures 1 and 2 show respectively a perspective view including the labeling scheme and a stereoscopic diagram of the molecule 3a. Interatomic distances and bond angles are listed in Tables VII and VIII, respectively. The molecule has ap-

(26) Bonnet, J.-J.; Lavigne, G.; Lugan, N.; Savariault, J. M., in preparation.

Table II. Positional and Thermal Parameters for the Atoms of $H_2Ru_3(CO)_6(P(C_6H_5)CH_2P(C_6H_5)_2)_2^a$

atom	x	y	z	$\beta(11)$	$\beta(22)$	$\beta(33)$	$\beta(12)$	$\beta(13)$	$\beta(23)$
Ru(1)	0	0.10140 (1)	1/4	47.2 (1)	22.09 (8)	21.32 (7)	0	-1.75 (7)	0
Ru(2)	0.09615 (1)	0.24610 (1)	0.284020 (9)	38.59 (9)	25.39 (6)	21.83 (5)	-0.32 (6)	0.17 (5)	-3.30 (4)
P(1)	0.01444 (4)	0.16271 (3)	0.36274 (3)	43.5 (3)	26.9 (2)	21.1 (2)	5.1 (2)	-1.3 (2)	0.8 (1)
P(2)	-0.14811 (4)	0.27336 (3)	0.33732 (3)	38.0 (3)	27.2 (2)	24.6 (2)	2.0 (2)	2.9 (2)	2.2 (1)
C(1)	0.1109 (5)	0.0441 (3)	0.2481 (3)	67 (4)	29 (2)	27 (2)	13 (2)	-5 (2)	-1 (2)
O(1)	0.1788 (3)	0.0084 (3)	0.2458 (2)	78 (3)	54 (2)	53 (2)	30 (2)	-4 (2)	-6 (2)
C(1b)	0.0735 (5)	0.0079 (4)	0.2459 (3)	89 (5)	29 (2)	27 (2)	3 (3)	-2 (2)	-1 (2)
O(1b)	0.1200 (4)	-0.0474 (3)	0.2434 (3)	140 (5)	45 (2)	50 (2)	45 (3)	6 (2)	2 (2)
C(2)	0.2103 (2)	0.2077 (2)	0.3191 (1)	52 (1)	39 (1)	38.6 (10)	10 (1)	3.4 (9)	0.2 (8)
O(2)	0.2804 (1)	0.1875 (1)	0.3408 (1)	57 (1)	73 (1)	69 (1)	26 (1)	-6.7 (9)	4.2 (9)
C(3)	0.1086 (2)	0.3425 (1)	0.3388 (1)	42 (1)	37.4 (10)	33.5 (8)	3.1 (9)	-5.3 (8)	-8.4 (7)
O(3)	0.1149 (1)	0.3990 (1)	0.3739 (1)	76 (1)	49.5 (9)	55.2 (7)	3.2 (9)	-11.5 (8)	-28.6 (8)
C(4)	-0.0894 (2)	0.2068 (1)	0.4043 (1)	51 (1)	35.6 (9)	27.2 (7)	7.3 (9)	4.7 (8)	5.7 (7)
C(5)	0.0745 (2)	0.1203 (1)	0.4423 (1)	43 (1)	42 (1)	23.0 (7)	7.0 (9)	0.4 (7)	4.3 (7)
C(6)	0.0938 (2)	0.0389 (2)	0.4439 (2)	80 (2)	43 (1)	41 (1)	1 (1)	-15 (1)	14.3 (9)
C(7)	0.1422 (3)	0.0051 (2)	0.5018 (2)	99 (2)	58 (2)	55 (1)	6 (2)	-18 (2)	26 (1)
C(8)	0.1689 (2)	0.0521 (3)	0.5598 (2)	72 (2)	96 (2)	37 (1)	16 (2)	-6 (1)	23 (1)
C(9)	0.1514 (3)	0.1312 (3)	0.5595 (2)	97 (3)	102 (3)	38 (1)	31 (2)	-26 (1)	-20 (1)
C(10)	0.1043 (3)	0.1662 (2)	0.4995 (2)	108 (2)	60 (2)	40 (1)	30 (2)	-28 (1)	-14 (1)
C(11)	-0.1324 (1)	0.3744 (1)	0.3748 (1)	37 (1)	30.4 (8)	32.8 (8)	1.7 (8)	1.7 (7)	-2.9 (7)
C(12)	-0.1321 (2)	0.3894 (2)	0.4501 (2)	88 (2)	39 (1)	34.6 (9)	-2 (1)	0 (1)	-5.1 (8)
C(13)	-0.1220 (3)	0.4670 (2)	0.4760 (2)	114 (3)	46 (1)	44 (1)	2 (2)	-8 (1)	-14 (1)
C(14)	-0.1121 (2)	0.5302 (2)	0.4291 (2)	89 (2)	36 (1)	64 (2)	-1 (1)	-3 (1)	-14 (1)
C(15)	-0.1127 (2)	0.5168 (2)	0.3558 (2)	96 (2)	31 (1)	54 (1)	-1 (1)	7 (1)	-0.2 (10)
C(16)	-0.1218 (2)	0.4393 (2)	0.3285 (1)	76 (2)	33.6 (10)	36.4 (10)	7 (1)	5 (1)	1.0 (8)
C(17)	-0.2705 (2)	0.2525 (1)	0.3509 (1)	42 (1)	38.5 (10)	27.2 (7)	-1.9 (9)	3.7 (7)	2.2 (7)
C(18)	-0.3024 (2)	0.1739 (2)	0.3466 (2)	58 (2)	44 (1)	46 (1)	-10 (1)	12 (1)	0.2 (9)
C(19)	-0.3958 (2)	0.1577 (2)	0.3493 (2)	68 (2)	64 (2)	50 (1)	-27 (2)	12 (1)	1 (1)
C(20)	-0.4574 (2)	0.2189 (3)	0.3551 (2)	46 (2)	89 (2)	70 (2)	-19 (2)	4 (1)	3 (2)
C(21)	-0.4270 (2)	0.2959 (3)	0.3599 (3)	43 (2)	75 (2)	107 (3)	7 (2)	4 (2)	3 (2)
C(22)	-0.3332 (2)	0.3135 (2)	0.3579 (2)	43 (1)	48 (1)	70 (2)	3 (1)	3 (1)	1 (1)
				$B, \text{\AA}^2$	atom	x	y	z	$B, \text{\AA}^2$
H(1)	0	0.306	1/4	4.0	H(13)	-0.123	0.478	0.529	7.2
H(2)	0.099	0.153	0.243	4.0	H(14)	-0.107	0.584	0.448	7.6
H(41)	-0.072	0.236	0.447	4.8	H(15)	-0.105	0.562	0.322	7.1
H(42)	-0.130	0.164	0.419	4.8	H(16)	-0.122	0.430	0.276	6.0
H(6)	0.072	0.005	0.403	5.9	H(18)	-0.258	0.130	0.341	6.1
H(7)	0.158	-0.052	0.501	7.5	H(19)	-0.417	0.102	0.347	7.2
H(8)	0.200	0.027	0.601	7.1	H(20)	-0.523	0.207	0.359	9.3
H(9)	0.174	0.165	0.600	8.3	H(21)	-0.472	0.340	0.365	9.6
H(10)	0.092	0.224	0.498	7.3	H(22)	-0.312	0.369	0.360	7.3
H(12)	-0.140	0.345	0.485	6.2					

^a Estimated standard deviations in the least significant figure(s) are given in parentheses in this and all subsequent tables. The form of the anisotropic thermal ellipsoid is $\text{Exp}[-(\beta(11)h^2 + \beta(22)k^2 + \beta(33)l^2 + 2\beta(12)hk + 2\beta(13)hl + 2\beta(23)kl)]$. Then quantities given in the table are the thermal coefficients $\times 10^4$.

Table IV. Positional and Thermal Parameters for the Nongroup Atoms of $(\mu\text{-H})_2\text{Ru}_3(\text{CO})_6((\text{C}_6\text{H}_5)_2\text{AsCH}_2)_2$ ^a

atom	x	y	z	$\beta(11)$	$\beta(22)$	$\beta(33)$	$\beta(12)$	$\beta(13)$	$\beta(23)$
Ru(1)	0.24992 (7)	0.35256 (4)	0.24594 (6)	4.83 (5)	2.24 (3)	2.15 (3)	0.15 (5)	0.09 (3)	-0.10 (4)
Ru(2)	0.33725 (6)	0.49898 (6)	0.28174 (4)	3.77 (5)	2.48 (5)	2.12 (3)	0.12 (4)	0.19 (3)	-0.18 (3)
Ru(3)	0.14588 (6)	0.49330 (6)	0.20763 (5)	3.76 (5)	2.54 (5)	2.23 (3)	0.07 (4)	0.17 (3)	0.21 (3)
As(1)	0.26314 (8)	0.41276 (8)	0.36515 (6)	4.42 (7)	2.63 (6)	2.04 (4)	0.43 (5)	0.08 (4)	0.04 (4)
As(2)	0.09117 (8)	0.52305 (8)	0.33267 (6)	4.06 (6)	2.74 (6)	2.55 (4)	0.31 (5)	0.43 (4)	0.11 (4)
As(3)	0.23384 (8)	0.41121 (8)	0.12605 (6)	4.44 (7)	2.57 (6)	2.09 (4)	-0.30 (5)	0.18 (4)	-0.19 (4)
As(4)	0.39439 (8)	0.52774 (7)	0.15910 (6)	3.92 (6)	2.78 (6)	2.49 (4)	-0.24 (5)	0.59 (4)	-0.01 (4)
C(1)	0.3573 (10)	0.2985 (9)	0.2488 (7)	8 (1)	6.5 (9)	2.6 (5)	3.3 (8)	-0.4 (6)	-0.8 (5)
O(1)	0.4264 (7)	0.2657 (6)	0.2497 (5)	9.8 (8)	6.6 (6)	6.2 (5)	3.9 (6)	-1.6 (5)	-1.5 (4)
C(2)	0.179 (1)	0.2612 (8)	0.2459 (6)	12 (1)	4.3 (7)	2.0 (4)	-1.8 (7)	-0.5 (6)	0.1 (4)
O(2)	0.1371 (8)	0.2036 (6)	0.2465 (5)	18 (1)	4.4 (5)	5.2 (4)	-5.6 (6)	0.4 (5)	0.2 (4)
C(3)	0.4483 (8)	0.4568 (7)	0.3130 (6)	5.3 (8)	3.8 (6)	2.6 (4)	0.8 (5)	0.2 (5)	-0.5 (4)
O(3)	0.5169 (6)	0.4341 (6)	0.3341 (5)	6.1 (6)	6.8 (6)	5.6 (4)	2.2 (5)	-1.2 (4)	0.5 (4)
C(4)	0.0352 (8)	0.4620 (7)	0.1638 (6)	5.0 (7)	3.2 (6)	3.6 (5)	-0.3 (5)	-0.1 (5)	0.4 (4)
O(4)	-0.0356 (6)	0.4433 (6)	0.1395 (5)	5.8 (6)	6.0 (5)	7.1 (5)	-1.7 (4)	-1.5 (4)	-0.1 (4)
C(5)	0.3527 (7)	0.5938 (8)	0.3349 (7)	3.5 (7)	3.2 (6)	3.4 (5)	0.0 (5)	0.4 (4)	-0.4 (5)
O(5)	0.3593 (6)	0.6503 (5)	0.3702 (5)	7.2 (6)	3.9 (5)	5.7 (4)	0.2 (4)	-0.4 (4)	-2.9 (4)
C(6)	0.1412 (8)	0.5903 (9)	0.1535 (7)	4.1 (7)	3.9 (7)	3.3 (5)	-0.5 (6)	-0.5 (5)	0.6 (5)
O(6)	0.1385 (7)	0.6454 (6)	0.1200 (6)	8.5 (7)	5.1 (6)	6.2 (5)	0.2 (5)	-0.5 (5)	3.6 (4)
C(7)	0.1508 (7)	0.4542 (7)	0.4053 (6)	5.7 (7)	3.9 (6)	2.6 (4)	0.8 (5)	0.3 (4)	0.9 (4)
C(8)	0.3346 (7)	0.4652 (7)	0.0805 (5)	4.5 (6)	3.6 (6)	2.1 (4)	-0.9 (5)	1.0 (4)	0.0 (4)

atom	x	y	z	atom	x	y	z
H(71) ^b	0.164	0.482	0.451	H(81) ^b	0.312	0.498	0.039
H(72) ^b	0.111	0.410	0.418	H(82) ^b	0.376	0.428	0.059

^a Estimated standard deviations in the least significant figure(s) are given in parentheses in this and all subsequent tables. The form of the anisotropic thermal ellipsoid is $\exp[-(\beta(11)h^2 + \beta(22)k^2 + \beta(33)l^2 + 2\beta(12)hk + 2\beta(13)hl + 2\beta(23)kl)]$. The quantities given in the table are the thermal coefficients $\times 10^3$. ^b $B = 3.0 \text{ \AA}^2$.

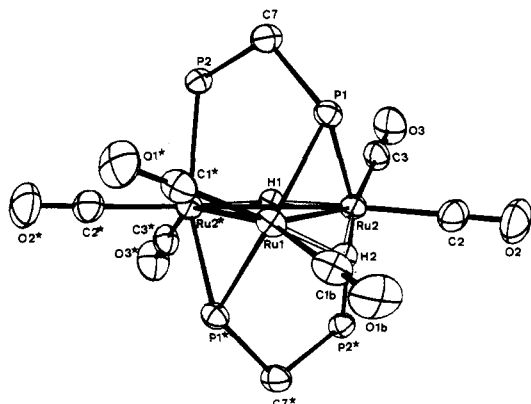


Figure 1. Perspective view of the complex $(\mu\text{-H})_2\text{Ru}_3(\text{CO})_6(\mu\text{-P}(\text{C}_6\text{H}_5)\text{CH}_2\text{P}(\text{C}_6\text{H}_5)_2)_2$ (3a). Phenyl rings about phosphorus atoms have been omitted for clarity. Vibrational ellipsoids are given at the 30% probability level.

parent crystallographic symmetry C_2 (vide infra) and consists of an isosceles triangle of metal atoms ($\text{Ru}(1)\text{-Ru}(2) = \text{Ru}(1)\text{-Ru}(2)^* = 2.8361(2) \text{ \AA}$; $\text{Ru}(2)\text{-Ru}(2)^* = 3.0367(5) \text{ \AA}$; $\text{Ru}(1)$ lies on the C_2 axis). Both cluster faces are capped in a similar way by identical ligand units $\mu\text{-P}(\text{C}_6\text{H}_5)\text{CH}_2\text{P}(\text{C}_6\text{H}_5)_2$ which are related by the C_2 symmetry operation. The first phosphorus atom $\text{P}(1)$ of a ligand unit bridges the $\text{Ru}(1)\text{-Ru}(2)$ edge ($\text{Ru}(1)\text{-P}(1) = 2.2958(6) \text{ \AA}$; $\text{Ru}(2)\text{-P}(1) = 2.3262(6) \text{ \AA}$) while the second phosphorus atom $\text{P}(2)$ is coordinated to $\text{Ru}(2)^*$ ($\text{Ru}(2)^*\text{-P}(2) = 2.3863(6) \text{ \AA}$) (Ru-P bond lengths are in the range of those observed in cluster species involving terminal²⁷⁻²⁹ or bridging^{1,30-32} phosphorus ligands). The same bonding situation

Table VII. Interatomic Distances (\AA) with Esd's for $(\mu\text{-H})_2\text{Ru}_3(\text{CO})_6(\mu\text{-P}(\text{C}_6\text{H}_5)\text{CH}_2\text{P}(\text{C}_6\text{H}_5)_2)_2$

Ruthenium-Ruthenium			
$\text{Ru}(1)\text{-Ru}(2)$	2.8361 (2)	$\text{Ru}(2)\text{-Ru}(2)^*$	3.0367 (5)
Ruthenium-Phosphorus			
$\text{Ru}(1)\text{-P}(1)$	2.2958 (6)	$\text{Ru}(2)^*\text{-P}(2)$	2.3863 (6)
$\text{Ru}(2)\text{-P}(1)$	2.3262 (6)		
Ruthenium-Carbon			
$\text{Ru}(1)\text{-C}(1)$	1.868 (6)	$\text{Ru}(2)\text{-C}(2)$	1.878 (3)
$\text{Ru}(1)\text{-C}(1b)$	1.881 (6)	$\text{Ru}(2)\text{-C}(3)$	1.888 (2)
Carbon-Oxygen			
$\text{C}(1)\text{-O}(1)$	1.150 (6)	$\text{C}(2)\text{-O}(2)$	1.135 (3)
$\text{C}(1b)\text{-O}(1b)$	1.139 (7)	$\text{C}(3)\text{-O}(3)$	1.135 (3)
Phosphorus-Carbon			
$\text{P}(1)\text{-C}(4)$	1.845 (2)	$\text{P}(2)\text{-C}(11)$	1.819 (2)
$\text{P}(1)\text{-C}(5)$	1.820 (2)	$\text{P}(2)\text{-C}(17)$	1.828 (2)
$\text{P}(2)\text{-C}(4)$	1.843 (2)		
Carbon-Carbon			
$\text{C}(5)\text{-C}(6)$	1.377 (3)	$\text{C}(11)\text{-C}(12)$	1.393 (3)
$\text{C}(6)\text{-C}(7)$	1.378 (4)	$\text{C}(12)\text{-C}(13)$	1.376 (4)
$\text{C}(7)\text{-C}(8)$	1.363 (5)	$\text{C}(13)\text{-C}(14)$	1.359 (4)
$\text{C}(8)\text{-C}(9)$	1.333 (5)	$\text{C}(14)\text{-C}(15)$	1.353 (4)
$\text{C}(9)\text{-C}(10)$	1.406 (4)	$\text{C}(15)\text{-C}(16)$	1.382 (3)
$\text{C}(10)\text{-C}(5)$	1.354 (3)	$\text{C}(16)\text{-C}(11)$	1.375 (3)
$\text{C}(17)\text{-C}(18)$	1.384 (3)	$\text{C}(20)\text{-C}(21)$	1.351 (5)
$\text{C}(18)\text{-C}(19)$	1.383 (4)	$\text{C}(21)\text{-C}(22)$	1.392 (4)
$\text{C}(19)\text{-C}(20)$	1.356 (5)	$\text{C}(22)\text{-C}(17)$	1.367 (3)

is, indeed, observed for the second ligand unit; it thus appears that the two equivalent ruthenium-ruthenium bonds $\text{Ru}(1)\text{-Ru}(2)$ and $\text{Ru}(1)\text{-Ru}(2)^*$ are supported by the bridgehead atoms $\text{P}(1)$ and $\text{P}(1)^*$, respectively, while the third one $\text{Ru}(2)\text{-Ru}(2)^*$ is unsupported. In keeping this, we originally expected to find the two hydride ligands bridging the two equivalent $\text{Ru}(1)\text{-Ru}(2)$ and $\text{Ru}(1)\text{-Ru}(2)^*$

(27) De Boer, J. J.; Van Doorn, J. A.; Masters, C. J. *Chem. Soc., Chem. Commun.* 1978, 1005.

(28) Forbes, E. J.; Goodhand, N.; Jones, D. L.; Hamor, T. A. *J. Organomet. Chem.* 1979, 182, 143.

(29) See also the X-ray structure of $\text{Ru}_3(\text{CO})_9(\text{dppm})_2\cdot 2(\text{CH}_3)_2\text{CO}$: Lavigne, G.; Lugan, N.; Bonnet, J.-J. *Acta Crystallogr., Sect. B* in press.

(30) Batarayan, K.; Zeolnai, L.; Huttner, G. *J. Organomet. Chem.* 1981, 209, 85.

(31) Iwasaki, F.; Mays, M. J.; Raithby, P. R.; Taylor, P. L.; Wheatley, P. J. *J. Organomet. Chem.* 1981, 213, 185.

(32) Natarayan, K.; Scheidsteger, O.; Huttner, G. *J. Organomet. Chem.* 1981, 209, 85.

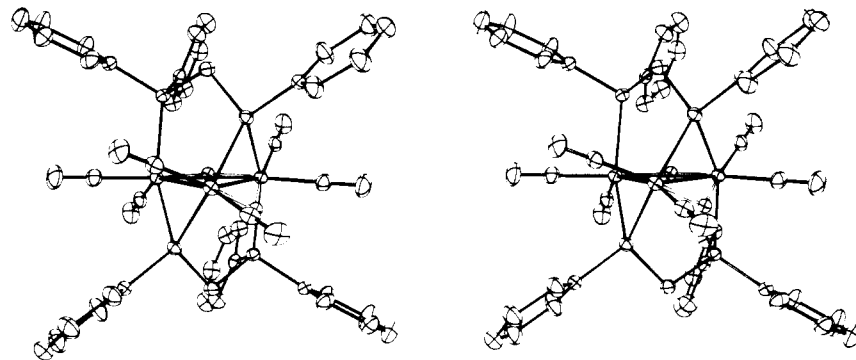


Figure 2. Stereoview of the complex $(\mu\text{-H})_2\text{Ru}_3(\text{CO})_6(\mu\text{-P}(\text{C}_6\text{H}_5)\text{CH}_2\text{P}(\text{C}_6\text{H}_5)_2)_2$ (**3a**).

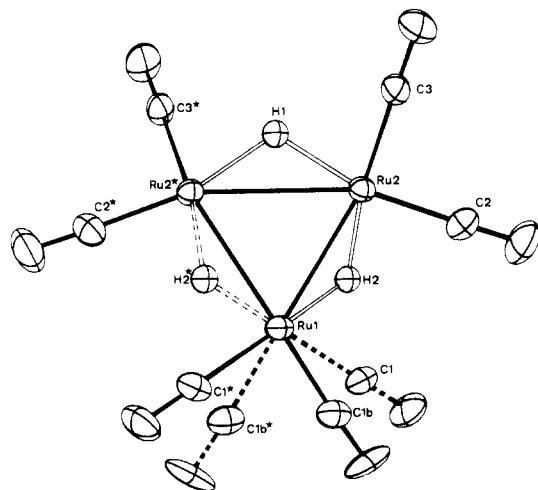


Figure 3. Distribution of carbonyl ligands in $(\mu\text{-H})_2\text{Ru}_3(\text{CO})_6(\mu\text{-P}(\text{C}_6\text{H}_5)\text{CH}_2\text{P}(\text{C}_6\text{H}_5)_2)_2$ (**3a**). The disorder of both carbonyl ligands bonded to Ru(1) is related to the alternate occupation of the two hydride sites H(2) and H(2)*.

(2)* bonds in addition to the bridging phosphorus atoms P(1) and P(1)*. Nevertheless, several important features give evidence for a different situation: (i) the ^1H NMR spectrum of **3a** in the high-field region shows two hydride multiplets ($\delta -15.87$ (1 H) $\delta -19.35$ (1H)) in agreement with the existence of two nonequivalent sites (vide infra); (ii) the highest peak in a tridimensional Fourier map is located on the C_2 axis, giving a reasonable position for the H(1) hydride ligand bridging the Ru(2)–Ru(2)* vector. This observation is fully consistent with the long bonding distance Ru(2)–Ru(2)* = 3.0367 (5) Å in agreement with the currently observed lengthening influence of a bridging hydride ligand.^{33,34} Consequently, the second hydride ligand could be expected to bridge one of the two equivalent metal–metal bonds available, i.e., Ru(1)–Ru(2) or Ru(1)–Ru(2)*, thus disturbing the crystallographic symmetry of the molecule. As shown in experimental part, a Fourier difference map allows an approximate location of this atom consistent with this assumption; (iii) finally, conclusive evidence for hydride location can be obtained from the orientations of equatorial carbonyl ligands which are depicted in Figure 3. The value of 107.20 (6)° found for both angles Ru(2)*–Ru(2)–C(3) and Ru(2)–Ru(2)*–C(3)* is significantly larger than the corresponding average Ru–Ru–CO (equatorial), 97.95°, in $\text{Ru}_3(\text{CO})_{12}$.³⁵ Such a

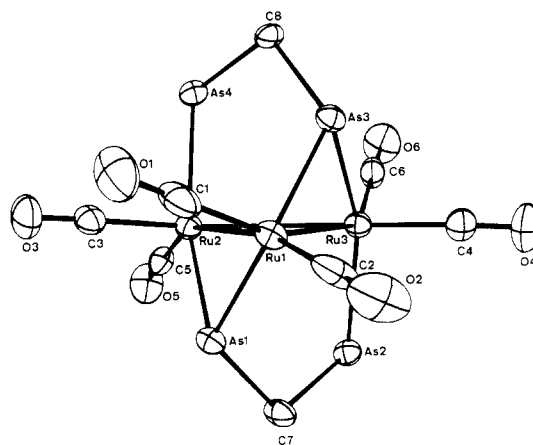


Figure 4. Perspective view of the complex $(\mu\text{-H})_2\text{Ru}_3(\text{CO})_6(\mu\text{-As}(\text{C}_6\text{H}_5)\text{CH}_2\text{As}(\text{C}_6\text{H}_5)_2)_2$ (**3b**). Vibrational ellipsoids are given at the 30% probability level. Phenyl rings about phosphorus atoms have been omitted for clarity.

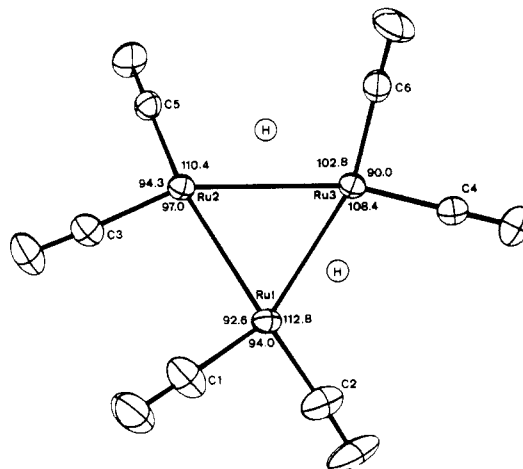


Figure 5. Distribution of carbonyl ligands in $(\mu\text{-H})_2\text{Ru}_3(\text{CO})_6(\mu\text{-As}(\text{C}_6\text{H}_5)\text{CH}_2\text{As}(\text{C}_6\text{H}_5)_2)_2$ (**3b**). The orientations of carbonyl ligands are well related to the presence of two hydride ligands bridging the metal–metal vectors Ru(1)–Ru(3) and Ru(2)–Ru(3).

perturbation is consistent with the presence of the bridging hydride H(1), in agreement with current observations in hydrido cluster complexes.^{36,37} The second μ -hydride ligand H(2) would be expected to induce similar repulsions about the adjacent carbonyl ligands. Accordingly, the disorder of the two carbonyl ligands bonded to Ru(1) (see Experimental Section) is related to the alternate occupation of the sites H(2) and H(2)*: the presence of a hydride in site H(2) is consistent with carbonyl groups C(1b)O(1b)

(33) Churchill, M. R.; De Boer, B. G.; Rotella, F. J. *Inorg. Chem.* 1976, 15, 1843 and references therein.

(34) Bau, R.; Koetzle, T. F.; *Pure Appl. Chem.* 1978, 50, 55 and references therein.

(35) Churchill, M. R.; Hollander, F. J.; Hutchinson, J. P. *Inorg. Chem.* 1977, 16, 2655.

(36) Churchill, M. R.; De Boer, B. G. *Inorg. Chem.* 1977, 16, 878.

(37) Jeannin, S.; Jeannin, Y.; Lavigne, G. *Inorg. Chem.* 1978, 17, 2103.

Table VIII. Bond Angles (Deg) with Esd's for $(\mu\text{-H})_2\text{Ru}_3(\text{CO})_6(\mu\text{-P}(\text{C}_6\text{H}_5)\text{CH}_2\text{P}(\text{C}_6\text{H}_5)_2)_2$

Within the Ru_3 Triangle			
$\text{Ru}(2)\text{-Ru}(1)\text{-Ru}(2)^*$	64.739 (9)	$\text{Ru}(1)\text{-Ru}(2)\text{-Ru}(2)^*$	57.630 (9)
Ru-Ru-P			
$\text{P}(1)\text{-Ru}(1)\text{-Ru}(2)$	52.63 (1)	$\text{P}(2)\text{-Ru}(2)^*\text{-Ru}(2)$	85.59 (2)
$\text{P}(1)\text{-Ru}(2)\text{-Ru}(1)$	51.67 (1)	$\text{P}(2)\text{-Ru}(2)^*\text{-Ru}(1)$	96.81 (1)
$\text{P}(1)\text{-Ru}(2)\text{-Ru}(2)^*$	77.16 (2)	$\text{P}(1)\text{-Ru}(1)\text{-Ru}(2)^*$	81.96 (2)
Ru-Ru-CO			
$\text{Ru}(2)\text{-Ru}(1)\text{-C}(1\text{b})$	115.2 (2)	$\text{Ru}(2)^*\text{-Ru}(2)\text{-C}(3)$	107.20 (6)
$\text{Ru}(1)\text{-Ru}(2)\text{-C}(2)$	102.56 (8)	$\text{Ru}(2)^*\text{-Ru}(1)\text{-C}(1)^*$	90.6 (2)
OC-Ru-CO			
$\text{C}(1)\text{-Ru}(1)\text{-C}(1\text{b})^*$	94.1 (3)	$\text{C}(2)\text{-Ru}(2)\text{-C}(3)$	91.65 (9)
P-Ru-C			
$\text{P}(1)\text{-Ru}(1)\text{-C}(1\text{b})$	110.7 (2)	$\text{P}(1)\text{-Ru}(1)\text{-C}(1)^*$	106.0 (2)
$\text{P}(1)^*\text{-Ru}(1)\text{-C}(1\text{b})$	111.9 (2)	$\text{P}(1)^*\text{-Ru}(1)\text{-C}(1)^*$	99.9 (2)
C-P-C			
$\text{C}(4)\text{-P}(1)\text{-C}(5)$	102.19 (9)	$\text{C}(4)\text{-P}(2)\text{-C}(17)$	103.8 (1)
$\text{C}(4)\text{-P}(2)\text{-C}(11)$	104.3 (1)	$\text{C}(11)\text{-P}(2)\text{-C}(17)$	103.9 (1)

Table IX. Interatomic Distances (Å) with Esd's for $(\mu\text{-H})_2\text{Ru}_3(\text{CO})_6(\mu\text{-As}(\text{C}_6\text{H}_5)\text{CH}_2\text{As}(\text{C}_6\text{H}_5)_2)_2$

Ruthenium-Ruthenium			
$\text{Ru}(1)\text{-Ru}(2)$	2.859 (2)	$\text{Ru}(2)\text{-Ru}(3)$	3.089 (2)
$\text{Ru}(1)\text{-Ru}(3)$	2.906 (1)		
Ruthenium-Arsenic			
$\text{Ru}(1)\text{-As}(1)$	2.451 (2)	$\text{Ru}(2)\text{-As}(4)$	2.523 (2)
$\text{Ru}(1)\text{-As}(3)$	2.454 (2)	$\text{Ru}(3)\text{-As}(3)$	2.470 (2)
$\text{Ru}(2)\text{-As}(1)$	2.428 (2)	$\text{Ru}(3)\text{-As}(2)$	2.555 (2)
Ruthenium-Carbon			
$\text{Ru}(1)\text{-C}(1)$	1.83 (1)	$\text{Ru}(2)\text{-C}(5)$	1.90 (1)
$\text{Ru}(1)\text{-C}(2)$	1.87 (1)	$\text{Ru}(3)\text{-C}(4)$	1.87 (1)
$\text{Ru}(2)\text{-C}(3)$	1.86 (1)	$\text{Ru}(3)\text{-C}(6)$	1.93 (1)
Carbon-Oxygen			
$\text{C}(1)\text{-O}(1)$	1.16 (2)	$\text{C}(4)\text{-O}(4)$	1.16 (1)
$\text{C}(2)\text{-O}(2)$	1.15 (2)	$\text{C}(5)\text{-O}(5)$	1.16 (2)
$\text{C}(3)\text{-O}(3)$	1.14 (1)	$\text{C}(6)\text{-O}(6)$	1.12 (2)
Arsenic-Carbon			
$\text{As}(1)\text{-C}(7)$	1.97 (1)	$\text{As}(2)\text{-C}(21)$	1.927 (6)
$\text{As}(2)\text{-C}(7)$	1.97 (1)	$\text{As}(2)\text{-C}(15)$	1.932 (7)
$\text{As}(3)\text{-C}(8)$	1.97 (1)	$\text{As}(3)\text{-C}(27)$	1.973 (6)
$\text{As}(4)\text{-C}(8)$	1.99 (1)	$\text{As}(4)\text{-C}(33)$	1.919 (7)
$\text{As}(1)\text{-C}(9)$	1.961 (7)	$\text{As}(4)\text{-C}(39)$	1.943 (7)

and $\text{C}(1)\text{*O}(1)\text{*}$ ($\text{Ru}(2)\text{-Ru}(1)\text{-C}(1\text{b}) = 115.2 (2)^\circ$); alternatively, occupation of site $\text{H}(2)\text{*}$ is consistent with carbonyl groups $\text{C}(1)\text{O}(1)$ and $\text{C}(1\text{b})\text{*O}(1\text{b})\text{*}$. Consequently, in a given molecule, **3a**, the C_2 symmetry works for the whole molecule but the hydride $\text{H}(2)$ and related carbonyl groups bonded to $\text{Ru}(1)$.

B. Structure of 3b. The crystal structure of **3b** consists of the packing of four discrete trinuclear molecules per unit cell. A perspective view of a molecule, **3b**, is shown in Figure 4; it includes the labeling scheme which is somewhat different from that one used for **3a** owing to the fact that in **3b** all atoms are in general positions. Interatomic distances and bond angles are presented in Tables IX and X, respectively. Although a close similarity with **3a** can be observed, the main features to note are the following ones: (i) the molecule has no crystallographic symmetry; (ii) no disorder of carbonyl groups is now observed; (iii) the position of carbonyl ligands (see Figure 5) agrees well with previous observations that the two hydride ligands bridge the inequivalent metal-metal bonds $\text{Ru}(1)\text{-Ru}(3)$ and $\text{Ru}(2)\text{-Ru}(3)$. Indeed, $\text{Ru-Ru-C}(\text{O})$ angles adjacent to the hydride positions are significantly larger than others (see Table X); (iv) the ruthenium triangle is no longer isosceles, since ruthenium-ruthenium bond lengths in **3b** are well related to the presence of hydride

90MHz

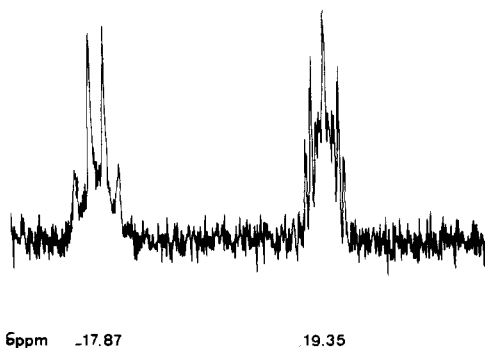


Figure 6. ^1H NMR spectrum of the complex **3a** in the high-field region showing two hydride resonances with superimposed phosphorus coupling.

ligands. A comparison of various Ru-Ru bonds in **3a** and **3b** is given:

3a		3b	
	2.8361 (2) Å		2.859 (2) Å
	2.8361 (2) Å		2.906 (1) Å
	3.0367 (5) Å		3.089 (2) Å

Although a lengthening influence is currently assigned to a bridging hydride ligand, the above table supports the previous observation³⁸ that metal-metal bond lengths in dibridged species M-X-M-H are also dependent on the nature of the bridgehead atom X.

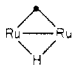
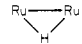
Structures of 3a and 3b in Solution. Despite the reported differences in the solid state, both dihydride species **3a** and **3b** were found to have a similar behavior in solution. Considering the complexity of phosphorus coupling in ^1H NMR spectrum of **3a** (see Figure 6), the problem was first elucidated with the arsenic derivative. Complete ^1H NMR data are displayed in Table XI. The ^1H NMR spectrum of **3b** also appears in Figures 7 and 8. The occurrence of two signals in the high-field region ($\delta -16.08, -20.11$) is consistent with the existence of two inequivalent bridging hydrido ligands. Such a disturbance

(38) Churchill, M. R.; Wasserman, H. J. *Inorg. Chem.* 1981, 20, 2905 and references therein.

Table X. Bond Angles (Deg) with Esd's for $(\mu\text{-H})_2\text{Ru}_3(\text{CO})_6(\mu\text{-P}(\text{C}_6\text{H}_5)\text{CH}_2\text{P}(\text{C}_6\text{H}_5)_2)_2$

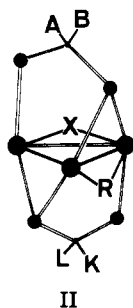
		Within the Ru ₃ Triangle	
Ru(1)-Ru(2)-Ru(3)	58.34 (4)	Ru(3)-Ru(1)-Ru(2)	64.79 (4)
Ru(2)-Ru(3)-Ru(1)	56.87 (3)		
Ru-Ru-As			
As(1)-Ru(1)-Ru(2)	53.75 (3)	As(4)-Ru(2)-Ru(1)	96.80 (4)
As(1)-Ru(1)-Ru(3)	84.50 (4)	As(4)-Ru(2)-Ru(3)	86.04 (5)
As(3)-Ru(1)-Ru(2)	83.58 (4)	As(3)-Ru(3)-Ru(1)	53.57 (4)
As(3)-Ru(1)-Ru(3)	54.08 (4)	As(3)-Ru(3)-Ru(2)	78.60 (4)
As(1)-Ru(2)-Ru(1)	54.50 (4)	As(2)-Ru(3)-Ru(1)	96.85 (4)
As(1)-Ru(2)-Ru(3)	80.98 (4)	As(2)-Ru(3)-Ru(2)	84.26 (4)
Ru-Ru-CO			
Ru(2)-Ru(1)-C(1)	92.6 (5)	Ru(1)-Ru(2)-C(3)	97.0 (4)
Ru(3)-Ru(1)-C(2)	112.8 (5)	Ru(3)-Ru(2)-C(5)	110.4 (3)
Ru(1)-Ru(3)-C(4)	108.4 (4)	Ru(2)-Ru(3)-C(6)	102.8 (3)
OC-Ru-CO			
C(1)-Ru(1)-C(2)	94.0 (7)	C(4)-Ru(3)-C(6)	90.0 (5)
C(3)-Ru(2)-C(5)	94.3 (5)		
As-Ru-C			
C(1)-Ru(1)-As(1)	98.3 (4)	C(3)-Ru(2)-As(1)	88.9 (4)
C(1)-Ru(1)-As(3)	106.3 (4)	C(3)-Ru(2)-As(4)	92.2 (3)
C(2)-Ru(1)-As(1)	111.6 (4)	C(5)-Ru(2)-As(1)	102.7 (4)
C(2)-Ru(1)-As(3)	107.6 (4)	C(5)-Ru(2)-As(4)	106.0 (4)
C-As-C			
C(21)-As(2)-C(15)	103.8 (4)	C(33)-As(4)-C(39)	101.6 (4)
C(21)-As(2)-C(7)	100.8 (4)	C(33)-As(4)-C(8)	101.7 (4)
C(15)-As(2)-C(7)	102.2 (4)	C(39)-As(4)-C(8)	102.4 (4)
C(8)-As(3)-C(27)	101.4 (4)	C(9)-As(1)-C(7)	100.9 (4)

Table XI. Summary of ¹H NMR Data^a

complexes	methylene signals	hydride signals		coupling const, Hz		
				$J_{\text{H-H}}^b$	$J_{\text{H-H}}^c$	$J_{\text{H-H}}^d$
1a	4.11 (4 H, t)					
3a	4.78 (2 H, br), 3.47 (2 H, br)	-17.87 (1 H, br)	-19.35 (1 H, br)			
1b	3.81 (4 H, s)					
1b*	4.57 (4 H, s)		-19.45 (1 H, s)			
2b	4.64 (2 H, s), 2.24 (2 H, q)	-14.56 (1 H, s)		11.3		
2b*	4.06 (2 H, q*), 2.93 (2 H, q)	-14.05 (1 H, d)	-18.49 (1 H, dd)	13.2, 12.1	2.2	1.4
3b	4.74 (2 H, q), 3.13 (2 H, q*)	-16.08 (1 H, dd)	-20.11 (1 H, d)	12.5, 11.7	3.6	2.2
3b*	3.75 (4 H, q*)	-16.18 (2 H, d)	-19.43 (1 H, s)	13.2	3.6	very weak

^a Chemical shifts are in ppm relative to internal Me₄Si. br = broad resonance; s = singlet; d = doublet; dd = doublet of doublet; q = quartet; q* = quartet with superimposed hydride coupling (see text). ^b Methylene. ^c Methylene-hydride. ^d Hydride-hydride.

on the symmetry of the molecule induces a magnetic inequivalence of the two methylene groups; it supports our treatment of this system with the labeling shown in II.



Features in the ¹H NMR spectrum of 3b (Table XI) can be discussed as follows: (i) the existence of an AB quartet for the first methylene resonance (δ 4.74 (2 H, $J_{\text{AB}} = 12.5$ Hz)) is consistent with the magnetic inequivalence of H nuclei within this group; (ii) a more intricate figure is found for the second methylene resonance KL (δ 3.13 (2 H, $J_{\text{KL}} = 11.7$ Hz)) since the left part of the observed quartet is split (Figure 7). This feature would suggest that K is

coupled to an additional nucleus (vide infra); (iii) in the high-field region, the hydride nucleus X is coupled to the second hydride nucleus R (δ -20.11 (d, 1 H, $J_{\text{RX}} = 2.2$ Hz); (iv) although a doublet would also be expected for the second hydride nucleus R, this resonance arises as a doublet of doublets (δ -16.08 (1 H)).

The occurrence of features ii and iv strongly suggest that the hydride nucleus R is coupled to the methylene proton K ($J_{\text{KR}} = 3.6$ Hz). A selective irradiation of R has proved to restore a symmetric quartet for the resonance of the methylene protons KL. Moreover a simulation of the entire ¹H spectrum has been performed by using the procedure described elsewhere:³⁹ it fits well with the observed one and shows features in good agreement with structural data; i.e., the hydride ligand X lies in the plane of the ruthenium triangle being thus far away from both methylene groups. In contrast, the hydride ligand R is bridging a ruthenium-ruthenium bond which is also supported by the bridgehead arsenic atom; this situation brings the hydride ligand R out of the plane of the ru-

(39) Bothner-By, A. A.; Castellano, S. "Quantum Chemistry Program Exchange"; Indiana University: Bloomington, IN, 1900; No. III.

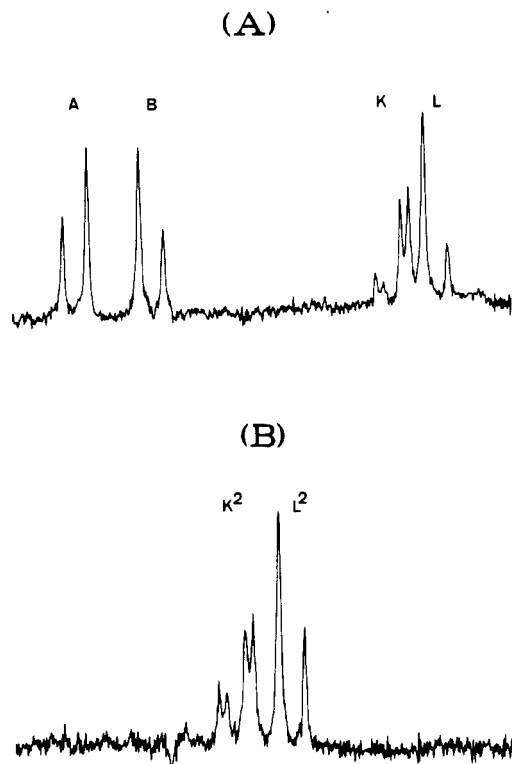


Figure 7. ^1H NMR spectra in the methylene region. (A) Complex $(\mu\text{-H})_2\text{Ru}_3(\text{CO})_6(\mu\text{-As}(\text{C}_6\text{H}_5)\text{CH}_2\text{As}(\text{C}_6\text{H}_5)_2)_2$ (**3b**): δ 4.74 (2 H, AB, q, $J_{\text{AB}} = 12.5$ Hz), δ 3.13 (2 H, KL, quartet with superimposed hydride coupling KR, $J_{\text{KL}} = 11.7$ Hz, $J_{\text{KR}} = 3.6$ Hz). (B) Complex $[(\mu\text{-H})_2\text{Ru}_3(\text{CO})_6(\mu\text{-As}(\text{C}_6\text{H}_5)\text{CH}_2\text{As}(\text{C}_6\text{H}_5)_2)_2]^+$ (**3b***): δ 3.75 (4 H, K^2L^2 , quartet with superimposed hydride coupling K^2R^2 $J_{\text{KL}} = 13.2$ Hz, $J_{\text{KR}} = 3.6$ Hz).

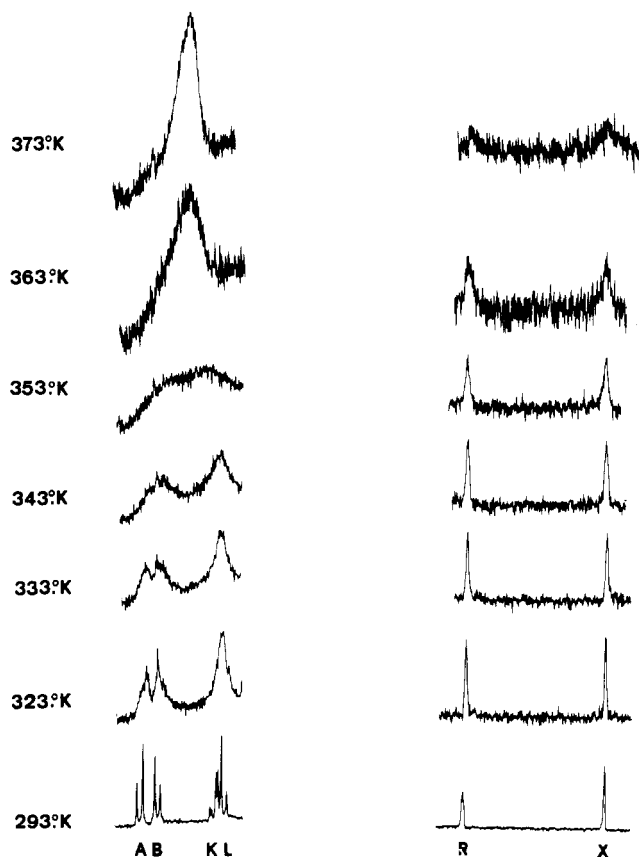


Figure 8. ^1H NMR spectrum of **3b**: variable-temperature experiment showing the coalescence of methylene signals at 360 K (same experiment with complex **3a** shows coalescence at 320 K).

thenium triangle, thus favoring the observed interaction which we believe to be a through-space coupling.

Two additional experiments were performed in order to check the correctness of this interpretation. First, a variable-temperature ^1H NMR experiment provided information on the mobility of hydride ligands. As shown in Figure 8, no exchange between R and X is observable on the NMR time scale, since no coalescence of hydride signals occurs in the temperature range 293–373 K. However, coalescence of the two methylene signals occurs at 360 K, clearly indicating a fast exchange of R between the two equivalent sites available to it. Same experiment performed with the phosphorus derivative **3a** showed the coalescence of the methylene signals at 320 K. In both cases, an edge-terminal-edge scrambling pathway involving thus a terminal hydride intermediate may work; evidence of such a process would require a variable-temperature ^{13}C experiment which has not been realized, owing to the low solubility of the complex.

If the inequivalence of the two methylene groups AB and KL is only related to the position of the hydride nucleus R, then occupation of the available site (R^*) by an additional proton should restore a perfect equivalence of both methylene signals. This was the main purpose of the second experiment which was realized upon acidification of **3b** with trifluoroacetic acid providing the cation $[(\mu\text{-H})_3\text{Ru}_3(\text{CO})_6(\mu\text{-As}(\text{C}_6\text{H}_5)\text{CH}_2\text{As}(\text{C}_6\text{H}_5)_2)_2]^+$ (**3b***). The ^1H NMR spectrum of **3b***, displayed in Table XI shows features which allow the following conclusions. (i) The integration of hydride signals shows a ratio 2/1, indicating that the additional nucleus occupies a site R^* equivalent to R (δ -16.18 (d, 2 H)). The very weak coupling R-X is not observable in this spectrum. (ii) The additional hydride nucleus R^* interacts with the methylene AB group in a way similar to the already observed interaction of R with KL. Consequently, both methylene resonances are no longer discernible and arise as a quartet K^2L^2 , the left part of which is split (Figure 7; δ 3.75 (4 H, δ 3.75 $J_{\text{KL}} = 13.2$ Hz, $J_{\text{KR}} = 3.6$ Hz)). It should be noted that the chemical shift of the methylene signal in **3b*** is close to the value observed when coalescence of the two signals occurs at 360 K for **3b**. (iii) This spectrum allows an unambiguous assignment of the hydride resonances to the two different sites

available in **3b**, i.e., Ru-As-Ru-H and Ru-H-Ru . It thus appears that the effect of the bridgehead atom (As or P) is a lowering of the hydride resonance. Accordingly, acidification of the monohydride species **2b** (it has been proved by neutron diffraction²⁶ that in **2b** the hydride ligand occupies the site bridged by the arsenic atom) provides an upperfield resonance in agreement with the fact that the additional hydride ligand occupies one of the two unsupported ruthenium-ruthenium bonds (see Table XI).

The study of these complexes raises at least two intriguing questions. First, why in both complexes **3a** and **3b** a hydride ligand occupies a site related to a nonbridged metal-metal bond even though a site associated with a bridged metal-metal bond is available? Apparently, the latter site is not sterically hindered since it can be occupied by an additional hydrogen atom upon acidification. In regard to the preferred sites associated with metal-metal bonds $\text{Ru}(2)\text{-Ru}(2)^*$ in **3a** and $\text{Ru}(2)\text{-Ru}(3)$ in **3b**, we would suggest that the large bite angle of both rigid face capped ligands accounts in determining large metal-metal separations $\text{Ru}(2)\text{-Ru}(2)^* = 3.0367$ (5) Å in **3a** and $\text{Ru}(2)\text{-Ru}(3) = 3.089$ (2) Å in **3b**: this may lower the potential energy of the corresponding sites of bridging hydride ligands. Another important question concerns the mecha-

nism of these reactions. Since no quantitative oxidative cleavage of dppm or dpam ligands occurs when **1a** or **1b** are heated at 80–85 °C for 90 min, the oxidative addition of hydrogen has likely preceded the oxidative cleavage of the ligand. Is there any possibility to obtain activation of hydrogen without oxidative cleavage of dppm or dpam ligands? Such a reaction has not been observed until now. The oxidative addition of hydrogen seems to promote subsequent cleavage of these ligands; it also provides a satisfactory control of these reactions which do not go further: both complexes **3a** and **3b** were recovered unchanged after prolonged reflux in dibutyl ether (145 °C).

Preliminary Catalytic Runs. The hydrogenation of cyclohexanone was chosen as a first test, owing to the known efficiency of $H_4Ru_4(CO)_{12}$ and related phosphine derivatives for this reaction.⁷ The preliminary results mentioned here were obtained under experimental conditions close to those stated in the referenced paper:⁷ no attempt was made to check the influence of temperature and hydrogen pressure on the rate of the hydrogenation reaction. Although attempts to use **1a** as the loaded form of the catalyst gave poor conversion yields, direct use of the dihydride species **3a** led to satisfactory results. It should be noted that the rate of hydrogenation is lower than that obtained for $H_4Ru_4(CO)_{12}$. Nevertheless, the amount of 89.8% conversion after 18 h is close to the best results obtained by using phosphine-substituted derivatives of $H_4Ru_4(CO)_{12}$ under closely related experimental conditions.⁷ The important point, however, is that a degradation of the cluster frame of **3a** is avoided under the reported conditions. Indeed, after the hydrogenation reaction, the cluster **3a** could be recovered unchanged. This result supports previous design of nonfluxional face-bridging ligands in view of cluster catalysis,^{3,8} despite the known limited use of such complexes under extremely

severe conditions.⁴⁰ Following the previous demonstrations that a reversible opening of metal–metal bonds may have a role in cluster catalysis,^{41–44} we would suggest that the activity of **3a** could be related to the observed mobility of the hydride ligand providing active sites through a reversible opening of M–H–M bonds.

We are now exploring possible new applications of these complexes in catalysis. Some of these applications may be inferred from our recent observation⁴⁵ that the dihydrido cluster complexes can be synthesized through the reaction of **1a** or **1b** with water. We emphasize that investigators in catalysis with phosphine-substituted clusters should be aware of possible transformations of such complexes under catalytic conditions. Let us recall an earlier communication² concerning a hydroformylation of propene using $Rh_4(CO)_{10}(PPh_3)_2$ for which a catalytic reaction was observed together with decomposition of the phosphine.

Acknowledgment. Financial assistance from CNRS (ATP "Chimie Fine") and DGRST is gratefully acknowledged.

Registry No. **1a**, 77611-27-9; **1b**, 81875-88-9; **2b**, 81875-89-0; **3a**, 81875-90-3; **3b**, 81875-91-4; cyclohexanone, 108-94-1.

Supplementary Material Available: Table III, Table V, Table VI, and a listing of structure factor amplitudes for compounds **3a** and **3b** (47 pages). Ordering information is given on any current masthead page.

- (40) King, R. B.; King, A. D.; Tanaka, K. *J. Mol. Catal.* 1981, 10, 75.
 (41) Keister, J. B.; Shapley, J. R. *J. Am. Chem. Soc.* 1976, 18, 1056.
 (42) Deeming, A. J.; Hasso, S. *J. Organomet. Chem.* 1976, 114, 313.
 (43) Huttner, G.; Schneider, J.; Müller, H. D.; Mohr, G.; Von Seyerl, J.; Wohlfahrt, L. *Angew. Chem., Int. Ed. Engl.* 1979, 18, 76.
 (44) Ford, P. C. *Acc. Chem. Res.* 1981, 14 (2), 31.
 (45) Lavigne, G.; Brisson, C.; Bonnet, J.-J., unpublished results.

¹³C DNMR Study of [(Ph₃P)₂N][CoRu₃(CO)₁₃]. Evidence for a Unique Fluxional Process Which Involves Concerted Motion of 12 Carbonyl Ligands and Leads to Rapid Interconversion of Enantiomers

David A. Roberts, A. Dale Harley, and Gregory L. Geoffroy*

Department of Chemistry, The Pennsylvania State University, University Park, Pennsylvania 16802

Received April 7, 1982

A variable-temperature ¹³C NMR study has been conducted on [(Ph₃P)₂N][CoRu₃(CO)₁₃], a tetranuclear cluster with a chiral arrangement of carbonyl ligands. The spectral data indicate that the lowest energy exchange process involves concerted motion of 12 of the 13 carbonyls and leads to interconversion of the two enantiomers of the cluster anion.

The cluster anion [CoRu₃(CO)₁₃]⁻ has been shown by an X-ray diffraction study to adopt the unique structure shown in Figure 1 with carbonyls bridging each of the three Co–Ru bonds.^{1,2} These bridging carbonyls are positioned

such that each is nearly coplanar with one of the three CoRu₂ faces. Furthermore, as shown in Figure 2, the three terminal carbonyls on each Ru are nonequivalent. This

(1) Steinhardt, P. C.; Gladfelter, W. L.; Harley, A. D.; Fox, J. R.; Geoffroy, G. L. *Inorg. Chem.* 1980, 19, 332.

(2) The only other cluster known to have a distribution of CO ligands similar to that in [CoRu₃(CO)₁₃]⁻ is [FeRu₃(CO)₁₂(NO)]⁻: Fjare, D. E.; Gladfelter, W. L. *J. Am. Chem. Soc.* 1981, 103, 1572.